Experimental and Analytical Development of Health Management for Electro-Mechanical Actuators

Matthew J. Smith
Carl S. Byington, Matthew J. Watson
Sudarshan Bharadwaj, Genna Swerdon
Impact Technologies, LLC
State College, PA 16801
814-861-6273
Matthew.Smith@Impact-Tek.com

Kai Goebel, Edward Balaban
NASA Ames Research Center
Moffett Field, CA 94035
Kai.Goebel@nasa.gov

Abstract—Expanded deployment of Electro-Mechanical Actuators (EMAs) in critical applications has created much interest in EMA Prognostic Health Management (PHM), a key enabling technology of Condition Based Maintenance (CBM). As such, Impact Technologies, LLC is collaborating with the NASA Ames Research Center to perform a number of research efforts in support of NASA's Integrated Vehicle Health Management (IVHM) initiatives. These efforts have combined experimental test stand development, laboratory seeded fault testing, and physical model-based health monitoring in a comprehensive PHM system development strategy. This paper discusses two closely related EMA research programs being conducted by Impact and NASA Ames. The first of these efforts resulted in the creation of an electro-mechanical actuator test stand for the Prognostics Center of Excellence at the NASA Ames Research Center. The second effort is ongoing and is utilizing physics-based modeling techniques to develop an algorithm and software package toolset for PHM of aircraft EMA systems using a hybrid (virtual sensor) approach.[1,2]

TABLE OF CONTENTS

1. INTRODUCTION.....1
2. TEST STAND DESIGN.....2
3. TEST STAND COMPONENTS.....4
4. TEST STAND SOFTWARE.....7
5. PRELIMINARY TEST RESULTS.....7
6. MODEL-BASED PHM.....8
7. PRELIMINARY MODEL-BASED RESULTS.....10
8. CONCLUSIONS.....12
9. FUTURE WORK.....13
ACKNOWLEDGMENTS.....13
REFERENCES.....13
BIOGRAPHY.....13

1. INTRODUCTION

Electro-Mechanical Actuator (EMA) systems are currently employed in a wide variety of industries including: commercial aircraft, military air/land vehicles, robotics, and industrial process control. In recent years, EMAs have been adapted to many applications where conventional hydraulic actuators previously would have been used. Hydraulic actuators use a pressurized liquid medium supplied by a remote pump to transmit actuation power and perform work on linear or rotary mechanisms, while EMAs directly utilize electrical power to create motion. These devices generate controlled motion by way of a DC motor connected to a motion producing mechanism such as a ball-screw assembly or gear train.

A major advantage of electro-mechanical actuation is the elimination of the pumps, filters, hydraulic lines and other accessory components that are required for the generation and distribution of fluid power. A principle of cutting edge aircraft design known as power-by-wire, extends the practices of fly-by-wire to not only distribute aircraft control signals using electronic signals, but also provide all actuation power via electrical distribution as well. The weight reduction, maintenance advantages, and other appealing characteristics of power-by-wire have led to many research and development efforts aimed at expanding the role of EMAs in both military and commercial aircraft applications.[1],[2]

Aircraft actuation systems provide critical functionality in a variety of utility, propulsion system and flight control applications. Reliable and consistent function of actuators is vital for the safe, efficient and cost effective operation of the aircraft. Conventional actuator maintenance procedures often rely upon time-based service or replacement of fielded units. This approach in the worst case can result in loss of aircraft due to failure occurring before the end of the estimated component life span. However, since component

1
[1] 978-1-4244-2622-5/09/$25.00 ©2009 IEEE.
[2] IEEEAC paper #1591, Version 1, Updated October 31, 2008

life is generally estimated in a conservative manner to avoid catastrophic failure, maintenance actions are often performed when not warranted by the actual condition. Modern health monitoring techniques that provide an accurate diagnostic assessment of the current component health enable a transition to Condition Based Maintenance (CBM) where decisions to service or replace components are made according to the current estimated health state.

Prognostic Health Management (PHM) systems go beyond purely diagnostic approaches and estimate the progression of component degradation, thereby generating a continuously updated prediction of remaining component life. A PHM approach offers additional benefits beyond purely diagnostic systems by allowing advanced scheduling of maintenance procedures, proactive replacement part allocation, and enhanced fleet deployment decisions based upon the estimated progression of component life usage. Prior studies have demonstrated the process of applying PHM techniques to aircraft hydraulic actuator systems and the resulting benefits.[3],[4]. As the role of EMAs in aircraft applications continue to increase, PHM technologies will be a vital part of the Condition Based Maintenance strategy.

To increase the state-of-the-art in EMA PHM technology, Impact Technologies, LLC has performed multiple research efforts in support of work performed within the Controls and Dynamics Technology Branch at NASA Glenn Research Center (GRC) and the NASA Integrated Vehicle Health Management (IVHM) initiatives. These programs combine experimental test stand development, laboratory seeded fault testing and physical model-based health monitoring to create a comprehensive, synergistic PHM system development strategy.

Experimental efforts have resulted in the creation and testing of an Electro-Mechanical Actuator test stand for The Prognostics Center of Excellence at the NASA Ames Research Center. Flexible system design allows for testing and data collection for a wide variety of actuator sizes and configurations with minimal modification required. The test stand is configured for both long term degradation and seeded fault testing of actuators under resistive loads of up to 5 metric tons. An extensive sensor suite including high performance displacement sensors, accelerometers, thermocouples and load measurement provides a comprehensive picture of EMA response and current health state. A centralized control and data acquisition PC provides a flexible environment for test definition, execution and real-time PHM algorithm deployment.

Model-based PHM efforts have focused on developing and validating an algorithm and software package toolset for prognostics and health management (PHM) of aircraft EMA systems using a hybrid (virtual sensor) approach. This effort included creation of a detailed dynamic, component-level model of the system, built in a transportable simulation environment, to virtually sense parameters that can be used to detect degradation, isolate probable root cause, and assess severity. This simulation environment was also used as virtual test bed for performing fault insertion analysis to address initial algorithm development and experimental prioritization. The model-based predictor when coupled with failure mode diagnostics, advanced knowledge fusion, and failure mode progression (prognostic) algorithms within a probabilistic framework form a complete prototype EMA PHM solution. One of the system models applied to the PHM framework is designed to simulate the NASA Ames EMA Test Stand, creating the capability for a PHM design methodology that couples experimental testing and computer model simulation.

2. TEST STAND DESIGN

The experimental portion of the NASA/Impact collaboration was focused on the design, fabrication and delivery of a turn-key experimental EMA test stand. This experimental test stand was created to provide a highly instrumented platform for the characterization of EMA performance and degraded system behavior while allowing for the real-time deployment and testing of health monitoring algorithms. The following sections detail the test stand design and the capabilities of the completed system.

System Requirements

The NASA Ames EMA test stand was created according to the original system requirements outlined by the Ames Prognostics Center of Excellence, as well as supplementary system capability dictated by Impact's prior EMA test stand development experience. A listing of the major system requirements appears below:

1) The test stand must accommodate a Moog 883-023 actuator as the initial test specimen. However, the test stand mounting must be flexible to allow for testing of linear actuators of varying configurations and sizes, including units larger than the initial test specimen (up to 450 mm stroke).

2) The two actuators (test, load) are to be directly coupled with a minimum amount of compliance while still providing some allowance for shaft misalignment. Excessive compliance would compromise the ability to adequately control load.

3) The test stand must include a loading mechanism capable of producing 5 metric tons of force. This load generating device must be directly driven by electricity (i.e. not hydraulic or pneumatic).

4) A centralized PC based interface is to manage all test definition, system control, data acquisition and visualization functionality. This PC must have

sufficient resources to allow simultaneous execution of real-time PHM algorithms during testing.

5) The system is required to specify custom load and motion profiles and maintain feedback control on both parameters simultaneously. The torque limit of the test EMA is also to be specified by a time-series profile during testing.

6) Feedback sensors (load, position) are required for system control and to record the parameter values throughout testing.

7) The test EMA is to be instrumented with a number of specialized sensors to provide a high fidelity measurement of system response. These sensors include multiple accelerometers, temperature measurements, drive current and high resolution measurement of ball-screw nut position.

8) The actuator mounting structure must provide a high level of rigidity. Deflection under load must be minimized to avoid distorting the high resolution measurements being taken on the test specimen.

9) The test stand must include appropriate provisions to ensure the safety of the user and prevent damage to the test stand hardware. This includes software based warnings and alarms that take corrective action when unsafe rig operation is experienced, as well as a hardware based emergency cut-off switch to immediately shut-down test stand power regardless of the software state.

The following sections provide the detailed system requirements and the design decisions that were made to accommodate them.

System Design Overview

A diagram of the overall system design is shown in Figure 1 below. This illustration outlines the major system components of the final design. A workstation computer is used as a centralized interface for data acquisition/visualization and system control. The data acquisition (DAQ) system provides all digital and analog communication between the PC and the other system components. The proportional integral differential (PID) control loops that maintain the load and position levels are handled by an off-board microcontroller. A servo-drive is used to supply the amplified electrical power to each of the actuators. An in-line load cell and a linear position sensor are attached to the coupled actuator shafts and provide system feedback. The test specimen is instrumented with several additional sensors that provide a detailed indication of current system performance and provide evidence of the current health state.

The system diagram also outlines the major communication interfaces between each of the components. The central acquisition/control PC provides the interface to define all motion and load profiles. These profiles are communicated to the data acquisition system through the PCIe bus. The DAQ forwards the load and position setpoints to the external microcontroller, which then determines the appropriate command signal to send to each of the servo-drives based upon the system feedback sensors. The servo-drives receive position feedback from the embedded motor sensors, however to simplify control system design, the drives are configured to operate in open-loop mode. In this configuration the servo-drives are acting only as amplifiers for the control signal generated by the microcontroller. All system control is handled by the off-board two-axis microcontroller. This arrangement avoids conflicts that could occur between the control responses of nested PID loops. The signals produced by the feedback sensors and expanded test specimen sensor suite are acquired by the DAQ system hardware. All signals are communicated back to the central PC for visualization and storage purposes.

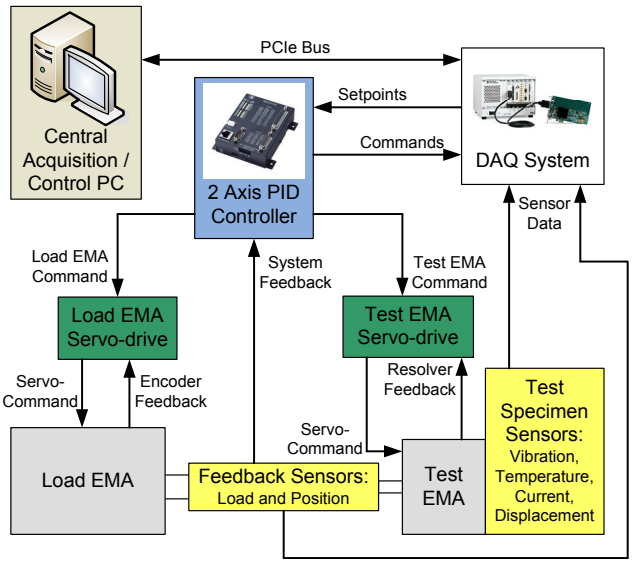

Figure 1 - EMA Test Stand System Diagram

Test Stand Hardware Overview

A photo of the NASA Ames EMA Test Stand is presented in Figure 2. The test stand hardware is distributed between three major system assemblies: the actuator mounting beam, power cart, and DAQ/PC rack.

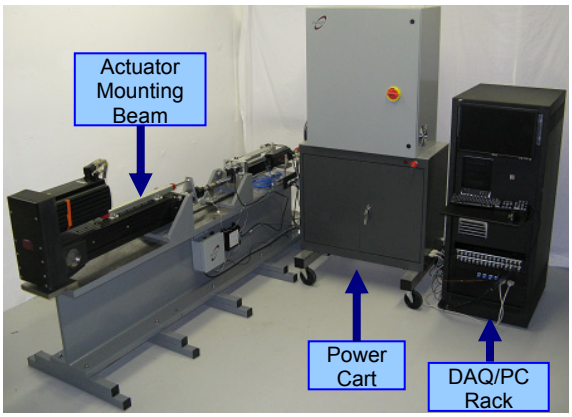

Figure 2 - EMA Test Stand Hardware

The actuator mounting beam provides mechanical support for both the load actuator and the test specimen. The structural steel I-beam utilized as the mounting surface has been sized well above the cross-sectional area required to survive the expected load levels. This design choice was made to provide extremely high bending rigidity since any significant deflection of the beam could distort the measurements of the high performance position sensor measurement. The beam surface has been precision ground to ensure alignment and stability of the mounting fixtures. The mounting beam is elevated and stabilized by five cross-members bolted to the lower flange. The actuators are each supported by a mounting bracket on the front and a compliant mount in the rear. The gusseted front L-bracket for each actuator is designed to carry the five metric ton maximum force generated by the load EMA with negligible deflection. The rear mounts provide no support in the direction of load, but reduce the long-term effect of the gravity moment created by the weight of each actuator. The load EMA (Moog 886) has been pre-aligned and shimmed and is intended as a permanent load fixture for the test stand. A mounting adaptor plate has been fabricated for the initial test specimen (Moog 883-023) to mate the actuator with the L-bracket. The flexible design of the mounting beam assembly allows for installation of test specimens of a wide variety of sizes and configurations. Mounting holes have been provided for front flange mounting of actuators at a variety of axial and vertical positions. Addition of a new test specimen to the assembly would require only the fabrication of a new mounting adaptor plate.

The other two major system assemblies contain the electrical components associated with power supply, system control and data acquisition. The power cart assembly contains the items that provide electrical supply to the actuators, sensors and other associated equipment. This includes the servo-drives for each of the two actuators and multiple 24 VDC power supplies dedicated to accessory equipment power supply and control signal purposes. Also, the PID controller that maintains the position and load setpoints during testing is located in this assembly. The DAQ/PC rack houses the test stand control computer and the data acquisition hardware (PXI chassis, breakout boards). This rack also mounts a monitor, mouse and keyboard.

3. Test Stand Components

The demanding requirements of the test stand required careful selection and specification of the system components. The following sections detail the selection process, specifications and capabilities of the major test stand hardware components.

Test Specimen

The initial EMA to be investigated on the test stand is a Moog Maxforce 883-023 unit. This actuator is a custom design that mates an 883 series ball-screw linear mechanism with a larger 4 series motor. The actuator is capable of producing 8.75 kN (1966 lbs) of continuous force, with a maximum continuous velocity of 125 mm/s (4.9 in/s). The unit has a total stroke of 305 mm (12 in) and utilizes an analog resolver for motor feedback. Several modifications have been performed on the test EMA to allow for the mounting of embedded sensors, including the creation of a slotting opening machined along the length of the actuator housing. Since this specimen was provided by the test stand program sponsor at NASA Ames, its configuration and capabilities guided the selection and specification of other components on the system.

The test EMA receives its control signal from a T200 series servo-drive. In the final system design, this unit is functioning in open-loop torque mode. While it is possible for the drive to accept resolver feedback and utilize that information to control motor motion, the internal loop has been disabled to stabilize system control response. In this case, the drive becomes an amplifier for the control signal dictated by the external two-axis controller. In addition to the torque command signal, the T200 can also accept a torque limit signal as an analog waveform. This functionality allows for the creation of custom torque limit profiles as specified in the test stand requirements. In addition to the analog input/output functions, the drive provides digital control bits that provide inputs to trigger drive actions and outputs to report the current drive status. An internal current sensor within the T200 is recorded by the data acquisition system as an indication of the current motor torque request. The test EMA can be seen along with the corresponding servo-drive in Figure 3.

Load Mechanism

A major requirement of the test stand was the generation of custom loading profiles of up to 5 metric tons using electrical power directly. This requirement eliminated hydraulic and pneumatic systems and pointed to the selection of a second, larger EMA as the loading mechanism. A second Moog Maxforce unit (886-9 series) was selected for the purpose of load generation. This unit meets the 5 ton load requirement with a continuous capacity of 52.16 kN (11726 lbs) and has a maximum continuous speed of 208 mm/s (8.18 in/s). A linear speed in excess of the test specimen capability is important to ensure that response rate of the load EMA will maintain load control when the test EMA is in motion.

The load EMA is driven by a Moog DS2110 servo-drive. As with the test specimen, the drive is operating in open-loop mode and acts as a control signal amplifier for the external two-axis controller. The DS2110 provides similar critical functionality as the test specimen drive, with one noted addition. While the system software provides continuous overload protection for the system, the internal drive current limiting functionality of the DS2110 provides the lowest-level line of defense to prevent test specimen damage. Using the drive, the absolute cut-off for load EMA motor torque can be adjusted according to the performance/safety needs of the current test. The load EMA can be seen along with the corresponding servo-drive in Figure 3.

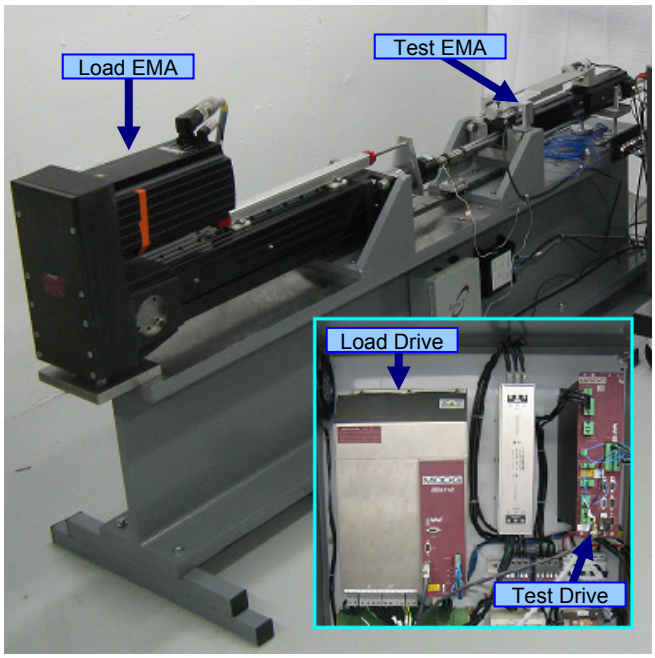

Figure 3 – Test/Load EMAs and Servo-Drives (Inset)

Two-Axis Controller

The system is continuously monitoring and maintaining specified position and load profiles. While it would be possible to perform the proportional integral differential (PID) calculations needed to generate the control signals for each iteration on the PC, these operations have been moved off-board to a two-axis microcontroller. This design decision frees up a significant computational resources to ensure the smooth operation of the test stand while simultaneously executing PHM algorithms, a functionality specified by the test stand requirements. The selected controller, a Galil RIO-47120, provides extensive digital and analog input/output (I/O) in addition to two real-time PID loops that can be programmed by an external PC. This device receives sensor feedback for load and position, sends a control signals to the test EMA drive to minimize the position error, and to the load EMA drive to minimize the load error. The controller's digital I/O capability is used to convert the 5v output bits generated by the data acquisition system to the 24v level required by the servo-drives.

Data Acquisition System

A National Instruments hardware package is utilized to manage digital and analog communication between the central PC and all other test stand hardware components. This includes generation of control setpoints, setting and clearing of digital control bits, monitoring of system status bits, and collection of all analog sensor data. Three data acquisition cards managed by a MXI Express Controller are used to provide this functionality. A PXI-6259 handles the generation of digital control bits, specification of the analog control signals, and acquisition of all low-speed sensor data. All high-speed (accelerometer) data is collected by a PXI-4472 card. A PXI-6521 industrial series card collects the 24v status bit information from both of the servo-drives. The default data collection rates are 1000 Hz for the low-speed data and 64 kHz for the accelerometers. In addition, the temperature data is processed by specialized thermocouple signal conditioning modules.

Central Control PC

A Dell workstation computer is used as the central interface to the test stand and is built around a 3.0 gHz dual-core Xeon processor. The specifications of the system were developed so as to provide an interface for all test definition, system control, and data acquisition and visualization while simultaneously functioning as a host for real-time PHM algorithms.

Feedback Sensors

An MTS magnetostrictive linear position sensor is connected to the coupled actuators by way of a mounting plate and monitors the current system motion. The sensor has been sized to accommodate actuators with stroke lengths of up to 450 mm (~18 in). Between the coupled actuators, a rod-end load cell has been installed to monitor the current load. The sensor is bi-directional and can report both compressive and tensile loading conditions. The location of the feedback sensors are shown in Figure 5.

Test Specimen Sensors

The initial EMA test specimen has been outfitted with a number of sensors that provide a high fidelity representation of current actuator performance. These sensors provide an enhanced picture of actuator health state that is not generally available with conventional EMA instrumentation. The presence of these measurements on the test stand allows for enhanced understanding of the nature of degraded EMA system response, as well as the ability to evaluate the benefit of added sensors on aircraft EMA system.

Temperature measurements are made in three locations within the actuator. Type T thermocouples are used, since their non-ferrous construction reduces the effect of surrounding electro-magnetic fields on the measurement. Thermocouples are attached to the inside of the motor housing near each of the two motor windings. These measurements provide the opportunity to detect irregular behavior within the motor and also provide an indication of how hard the EMA is working to overcome resistive loading. The third thermocouple is attached to the internal ball-screw nut surface and is targeted at failure mode conditions that instigate friction and heat generation with the ball screw mechanism.

Accelerometers take nine vibration measurements at five locations on the test specimen. The first two points are located on the centerline of the bottom surface of the actuator housing. Each of these locations is instrumented with a tri-axial ICP shear accelerometer manufactured by PCB. These sensors provide an indication of the bulk vibration of the EMA in the x, y and x planes. The other vibration measurements are targeted at the vibrations specific to the ball-screw nut assembly. A single axis ICP shear accelerometer is threaded into the outer surface of the ball-screw assembly and measures the overall vibration of the nut as it moves along the screw. In addition, embedded tear drop style shear ICP accelerometers have been affixed to the internal nut surface to better measure the subtle vibration pulses associated with motion of the ball elements. These accelerometers are mounted near the two topmost ball return channels inserts, which allow the rolling ball elements to travel from the end of the ball threads back to the beginning.

A failure mode of great interest to the EMA research group at NASA Ames is ball-screw assembly wear. As the actuator is subjected to repeated cycles, the surface of the screw can experience significant degradation that manifests itself by a subtle increase in the backlash experienced during cycle reversal. This backlash is measured by observing ball-screw nut motion that occurs with no corresponding motor motion. To capture this backlash event, a non-contact position sensor that can resolve relative motions as small as one micron (0.001 mm) is required. Investigation of current position sensing technologies indicated that only laser interferometer would have this fine level of resolution over the entire range of motion (~300 mm). This technology, due to its requirement for multiple precisely aligned components, was deemed impractical to implement in this application. Laser triangulation sensors meet the resolution requirement, but only over a smaller range of measurement (50 mm).

To address the high performance position sensing requirement, a two sensor solution was developed. In this arrangement, a Micro Epsilon Opto 2200-50 laser triangulation sensor is used to observe the backlash event over a reduced range of the actuator stroke. Since the sensor cannot be pointed directly at the ball-screw nut, a target assembly that stands on the top of the nut provides the surface of measurement. For a given test the laser sensor can be positioned by a precision linear slide assembly. The position of the laser sensor is reported by a magnetostrictive position sensor attached to the sliding bracket. This solution allows for trending of backlash along the entire length of the screw.

The externally visible components of the test specimen sensor suite are presented in Figure 4.

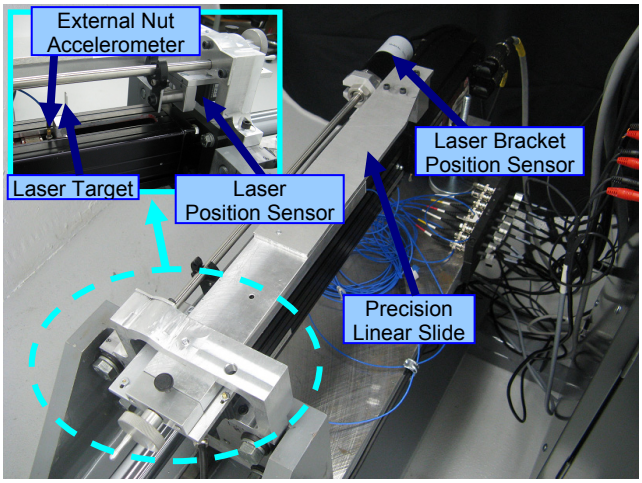

Figure 4 - Test Specimen Sensors

Mechanical Coupling Elements

In addition to the two feedback sensors (for load and position measurement), several other system components are threaded between the two coupled actuators. A rod-end coupling allows for lateral and spherical misalignment of the two EMAs, while introducing negligible axial compliance. It is critical to maintain high axial stiffness since deflection of the coupling would inhibit the ability of the system to maintain load control during stress reversal. The rod-end coupling allows for relative torsional displacement between the two threaded ends. This relative displacement enables the rotation required for the coupling and decoupling of the two actuators. Thread adaptors are required to mate the coupling and load cell to the rod-ends of each actuator. The custom part that mates the load EMA to the coupling is intended to be a permanent component of the test stand. The adaptor attached to the end of the test specimen would have to be replaced or supplemented to mate with the threads of a new test specimen. Since the current test EMA lacks internal anti-rotation control, and any motion in the rotational degree-of-freedom would distort the laser sensor measurement, a linear guide assembly has been attached to the test EMA thread adaptor. The mechanical coupling components are shown in Figure 5.

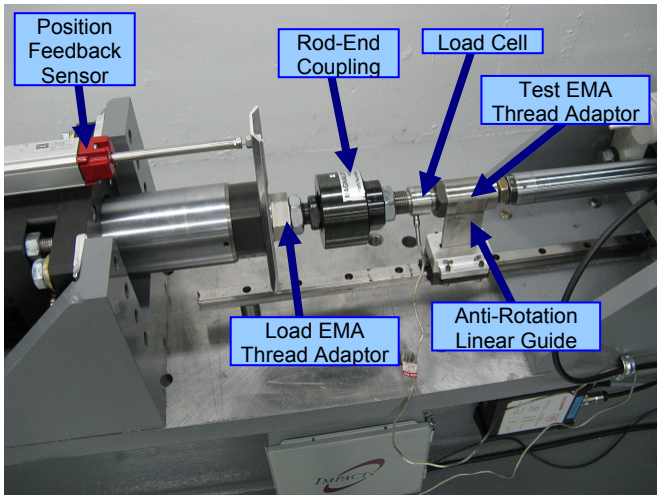

Figure 5 - Feedback Sensors and Coupling Components

Emergency Stop / System Switch

A 24 VDC control signal is used for the master system on/off switch. This electrical signal powers the coils in the three-phase contactors that switch the AC mains supplying each of the two actuators. When the 24 VDC signal is removed the contactors open and remove power to the servo-drives. The same electrical signal opens and closes a solid state relay that controls distribution of single-phase current to the accessory DC supplies that power the controller, sensors and other test stand hardware. The 24 VDC is interrupted by one of two means depending on the state of the rig. If a graceful shutdown is called for, the shut-down command in the test stand software interface is invoked and the 24 VDC signal is interrupted by a solid state relay according to predefined shutdown cycle. If unsafe or damaging test stand behavior is observed, the mechanical emergency stop switch is depressed to immediately discontinue all test stand activity.

4. Test Stand Software

The test stand software, developed in the National Instruments LabVIEW environment, is executed on the central test stand PC. The software provides the user interface for all test definition, system control and data visualization. The software also manages a system of warnings and alarms that notify the user of unsafe or undesirable system performance and, if warranted, shut down all test stand operation. Advanced configuration options allow administrators to configure the data collection options, perform maintenance motion operations, and manipulate warning and alarm thresholds. The interface panel provides real-time parameter values and component status information as well as the ability to plot up to eight data channels in real time. The main interface of the test stand software appears below in Figure 6.

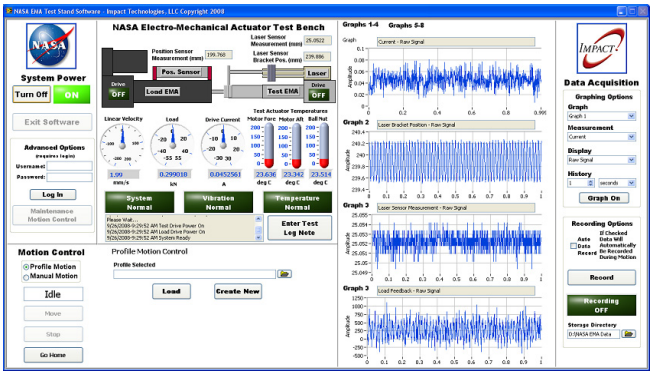

Figure 6 - Test Stand Software Main Interface

5. Preliminary Test Results

Initial EMA testing has commenced at the NASA Ames Research Center. Thus far, the testing has been performed with a known healthy specimen, but future tests are planned to investigate the response due to a variety of fault conditions. Also, Impact has planned testing to directly support the model-based PHM efforts discussed in this paper. Figure 7 provides sample data obtained from the test stand. The position and load command signals are presented

along with the corresponding feedback sensor measurements.

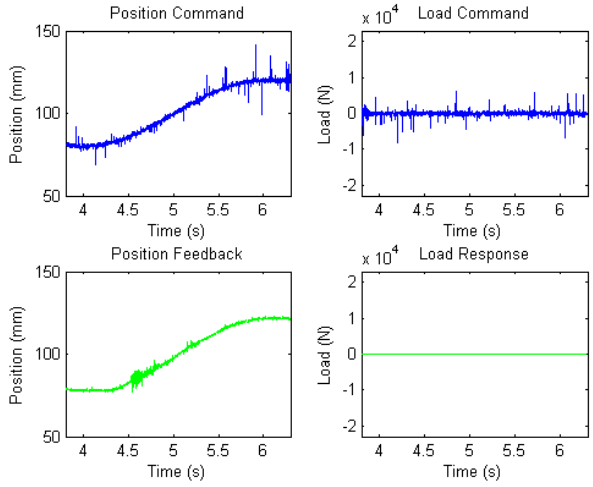

Figure 7 – Example Test Stand Response

6. MODEL-BASED PHM

The model-based approach to PHM (Figure 8) applies physical modeling and advanced parametric identification techniques. As an advantage over 'black-box' or purely data-driven health-monitoring schemes, faults and failure modes are traced back to physically meaningful system parameters, providing the maintainer with invaluable diagnostic information. The approach employs a mathematical dynamic model of the system that is directly tied to the physical processes that drive the health of the component. The control command is used on the model to simulate expected system response. The difference between the simulated and actual response is used to perform an estimation of system parameters (e.g., efficiency, friction factors, etc.). The estimated parameters are then compared with the baseline health level parameters to identify and isolate system faults and provide a measure of fault severity.

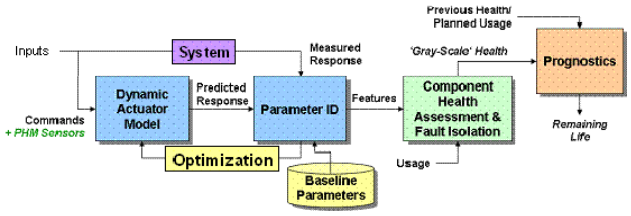

Figure 8 - Model-Based PHM Approach

To aid in the refinement of model-based PHM techniques for EMAs, a generalized dynamic system model of electro-mechanical actuators was developed. This model was created in the Simulink® environment of the MATLAB® software package, and can be employed to represent the physics of system degradation and its effects on the performance of components, systems or subsystems within the overall actuator system. To exercise this model under a variety of baseline and faulted conditions, a virtual test bed application was developed. The following sections detail these development efforts.

Dynamic System Model Development

A schematic of the general EMA system represented by the model is shown in Figure 9, while the developed EMA Simulink® model is shown in Figure 10.

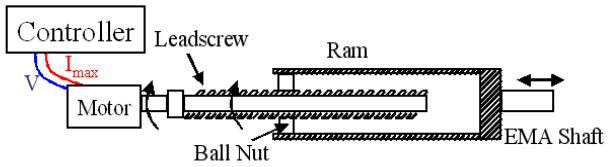

Figure 9 – Schematic of Electromechanical Actuator

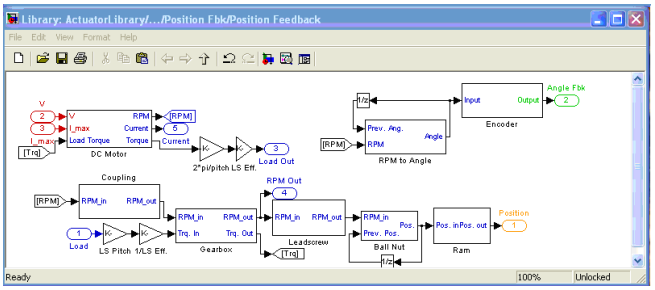

Figure 10 – Dynamic Model of Generalized EMA System

The model incorporates blocks for the various components within the EMA, such as the brushless DC motor, leadscrew and ball nut, ram, and output shaft. It also contains blocks for components such as the gearbox and encoder, which can be selected or deselected by the user, since these components may not be present on all EMAs. Similarly, the user may also select the type of control for the EMA, with the available choices being position control, velocity control, or torque control.

In addition, the model incorporates fault blocks within the various components. These blocks insert faults by modifying the control or feedback signals, or characteristic parameters within the component. Also, faults may be simulated by introducing biases or noise into actuator commands or measured responses.

The major assumptions made in creating this EMA model are listed below.

1) Brushless DC motor drives leadscrew

2) Each phase of motor is modeled as L-R circuit

3) Leadscrew, ball-nut, and ram modeled as rigid components with mechanical efficiencies

4) Shaft angular acceleration is proportional to excess torque (motor torque, less damping and load torques)

5) The motor is governed by the relationships shown in equations 1 to 3:

$$I_\phi = \frac{V_\phi}{R_\phi + L_\phi s} \quad [1]$$

$$\tau_\phi = k_{t_\phi} I_\phi \quad [2]$$

$$\tau_{Total} = J\ddot{\theta} + B\dot{\theta} + \tau_l \quad [3]$$

where I_ϕ is the current in each phase, V_ϕ is the voltage in each phase, R_ϕ is the winding resistance in each phase, L_ϕ is the winding inductance in each phase, τ is the motor torque, k_t is the torque constant, J is the rotor inertia, B is the damping on the rotor, and τ_l is the load torque acting on the rotor shaft.

In addition to the modeling of the electrical and mechanical parts of the EMA, a thermal model of the EMA motor was implemented. This model is described in Figure 11. As the figure shows, the model treats the motor windings as a lumped system, and determines their temperature at each time step based on the input heat (I^2R losses) and the heat lost to the surface of the motor. The motor surface in turn loses heat to the ambient air through convection and radiation.

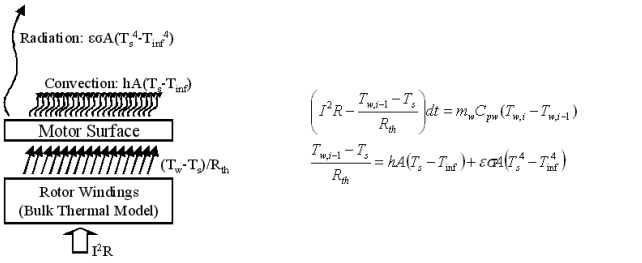

I	:	Winding Current	σ	:	Stefan's Constant
R	:	Winding Resistance	ε	:	Surface Emissivity
R_{th}	:	Thermal Resistance	T_s	:	Motor Surface Temperature
dt	:	Simulation Time Step	T_{inf}	:	Ambient Temperature
m_w	:	Mass of Windings	$T_{w,i-1}$	:	Winding Temperature at Timestep i-1
C_{pw}	:	Specific Heat of Windings			
h	:	Heat Transfer Coefficient	$T_{w,i}$	:	Winding Temperature at Timestep i
A	:	Motor Surface Area			

Figure 11 – Thermal Model of Actuator Motor

Virtual Test Bed Development

A virtual test bed environment was developed (also in Simulink®) to allow simulation of the developed model, critical faults, and other external effects (i.e., loads, control inputs, etc) that contribute to prediction uncertainty. This environment will be used to execute the validated model with various healthy and simulated fault conditions to produce a database of model parameters that characterize the response of the system. Since the initial target demonstration will be performed on NASA Ames' EMA Test Stand, a virtual test bed was constructed with this test stand in mind.

This test bed includes components to subject the test actuator to the desired load profiles, as well as to generate the control profiles (position, velocity, or torque) that define the motion of the actuator. In addition, the test rig also incorporates a variety of sensors to obtain and characterize the response of the actuator system to various external stimuli. These additional elements of the test rig are therefore also modeled in the virtual test bed environment. This environment serves the same purpose as the actual test bed environment, only the virtual environment operates in the digital realm to subject the actuator model to the required excitation profiles and loading environments. The developed virtual test bed environment therefore consists of a loading system, a controller, an actuator drive, and the required sensor blocks. Since the loading system was modeled as another EMA opposing the test EMA, an additional drive was also modeled for the load actuator. A block diagram of this test bed environment, showing the various control modes and feedback loops, is shown in Figure 12.

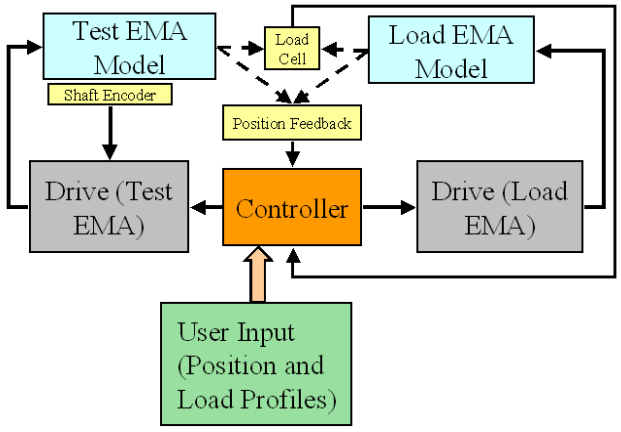

Figure 12 – Block Diagram of Virtual Test Bed Environment

As seen from the figure, a master controller sends command signals to the test and load control drives, which control the test and load EMAs, respectively. The command signals (from the drives to the EMAs) consist of voltage and current signals. The master controller receives feedback

from the position sensor, and sends out a control signal to the test EMA drive to correct for the current position error. The controller also receives a load feedback signal from the load cell sandwiched between the test and load EMA shafts. The controller sends a signal to the load EMA drive to minimize the load response error. A diagram of the actuator model within the virtual test bed environment is shown in Figure 13.

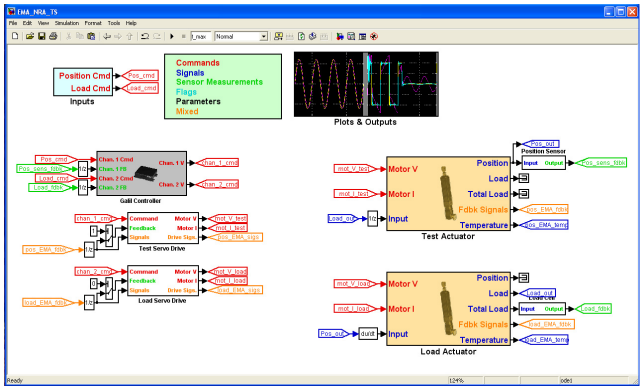

Figure 13 – Simulink® Virtual Test Bed Environment

7. Preliminary Model-Based Results

A number of simulations were performed in the virtual test bed environment. These simulations initially consisted of observation of the system response to various command inputs under expected healthy condition. The commands to the virtual test bed environment consisted of position and load profiles. For instance, Figure 14 shows the response of the test EMA to a sinusoidal position profile with a step change in the load. As seen, the controller and drive are able to maintain the specified position profile (top left plot in the figure) against the jump in the load. The bottom left plot in the figure shows a step change in the current drawn, corresponding to the change in the load (top right plot). The bottom right plot shows the temperature of the EMA motor windings and surface. As seen, the higher current draw from t=20 secs causes a faster rise in both temperatures.

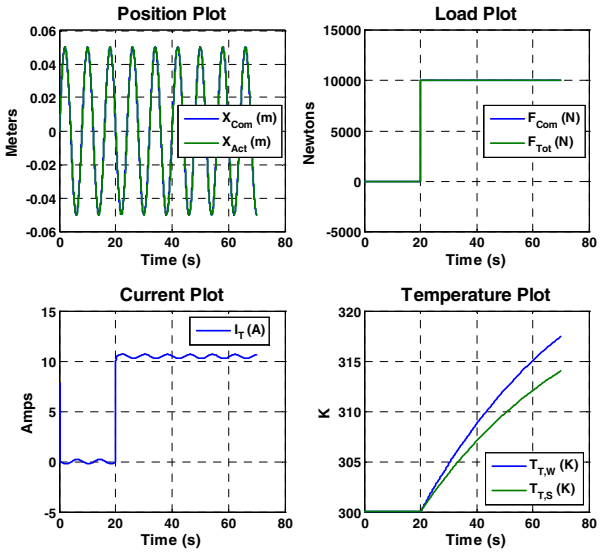

Figure 14 – Actuator Response to Sine Position and Step Load Profiles

Similarly, Figure 15 shows the response of the EMA to a position ramp command with a rectangular load cycle profile. Again, the controller and drive are able to maintain the specified ramp. The bottom left plot shows the current drawn by the EMA following the shape of the load profile (top right plot). The bottom right plot shows a steady motor RPM corresponding to the position ramp, except when the load rises or drops abruptly.

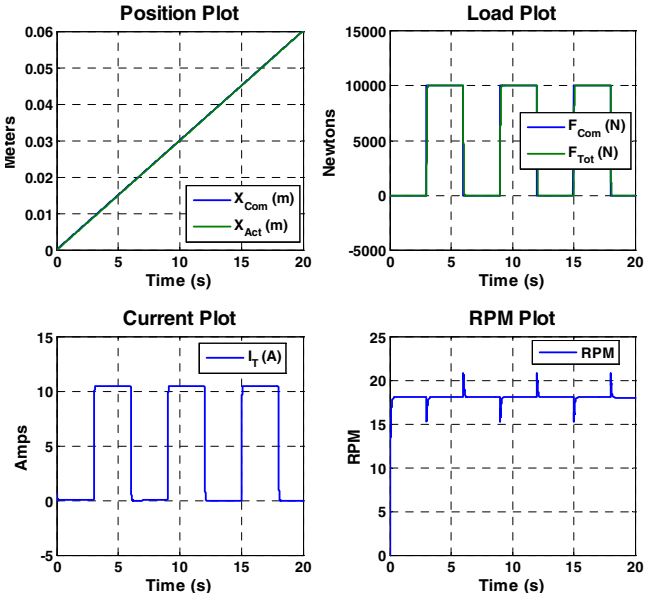

Figure 15 – Actuator Response to Ramp Position and Rectangular Load Profile

Once the response of the system to specified position and load profiles was verified, the next step was to conduct fault simulation tests using the model. These faults were modeled as gain, bias, and/or noise blocks on various parameters and signals within the model. For example, Figure 16 shows the simulation of a "loss of power to the motor" fault (see the

top half of the figure). This fault is simulated by specifying a gain on the motor command (without adding any bias or noise); in this case, the gain of zero simulates a complete (though temporary) loss of power to the motor. The bottom half of the figure shows the response of the EMA to a sinusoidal position profile with a steady load ramp, under the influence of this fault. As seen, the system is initially able to follow the position command (top left plot in bottom half of the figure). When motor power is lost, the test EMA goes dead. However, the load EMA is exerting a steady load against the test EMA in accordance with the specified load profile. This causes the test EMA to move backwards (shaft moves toward the body of the EMA). As the bottom left plot in the bottom half of the figure shows, there is still a current in the windings; however, this current is induced by the back EMF generated by the motion of the shaft, which forces the motor to turn (despite loss of power). Once the power is turned back on, the system resumes normal operation.

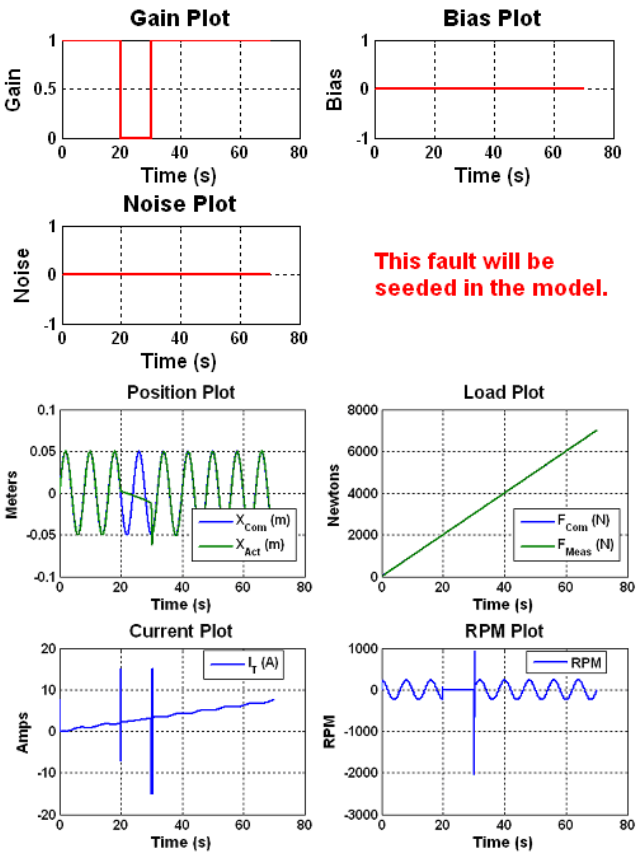

Figure 16 – EMA Response to Power Loss Fault

Similarly, a winding short was simulated in the motor by reducing the effective number of turns in the windings (Figure 17). This was achieved by placing a gain on the "number of turns" parameter (see top half of the figure). This parameter affects the motor winding resistance, the winding inductance, torque constant, and back EMF constant. The winding short was simulated in two phases: an initial mild fault, followed by a deteriorating fault that slowly recovers. The bottom half of the figure shows the response of the system to a sinusoidal position profile and rectangular load profile. As the bottom left plot in the bottom half of the figure shows, the initial mild winding short causes a rise in the current drawn by the motor, which compensates for the reduced torque constant (owing to the reduced effective number of windings). Since the motor is able to compensate for the fault, the actuator is still able to follow the specified position profile (top left plot in the bottom half of the figure). However, the maximum current that the motor can draw is limited by the drive. Thus, the later deteriorating winding short causes the motor to try and draw more current than the drive can supply. This limits the amount of compensation that the motor can provide against the fault, and the effect is seen in the position profile, where the load actuator overpowers the test EMA, causing it to deviate from the position command. Once the fault is removed, normal motion resumes.

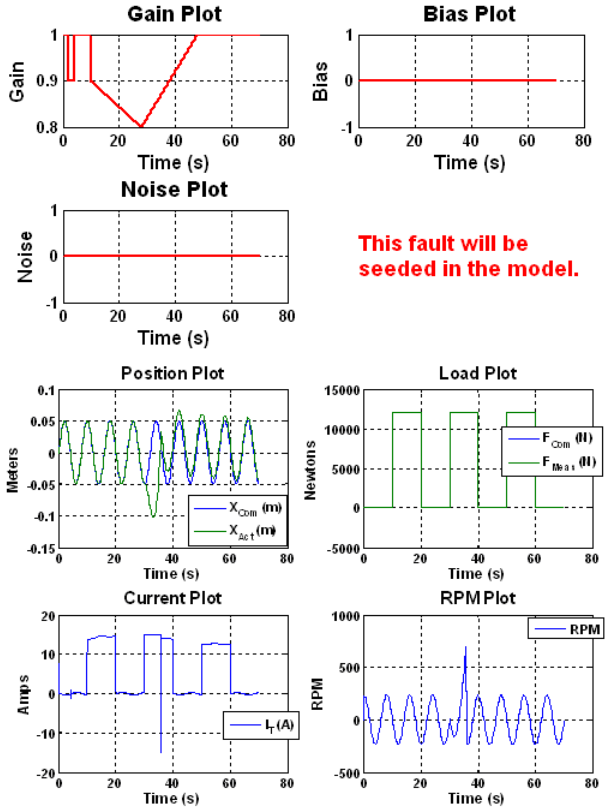

Figure 17 – EMA Response to Winding Short Fault

Once the response of the system to various simulated faults was analyzed and verified, the next step was fault diagnosis. This was achieved by deriving features from the actuator signals and correlating these features to fault severity levels. For example, the effective number of motor windings may be derived from the motor current and voltage signals through least squares optimization. This "effective number of winding turns" parameter is then used to diagnose the severity of the fault. This is illustrated in Figure 18. As seen, the parameter is able to provide an accurate estimate

of fault severity. Also of interest is the fact that the initial mild fault does not cause any significant deviation of the measured position from the commanded position, despite which the derived feature is still able to estimate the severity of the fault. As explained previously, the later, deteriorating winding short causes current limiting circuitry within the drive to enter the picture, which is why the position response of the EMA is affected. This initially throws off the diagnostic feature, but fault estimation accuracy subsequently recovers.

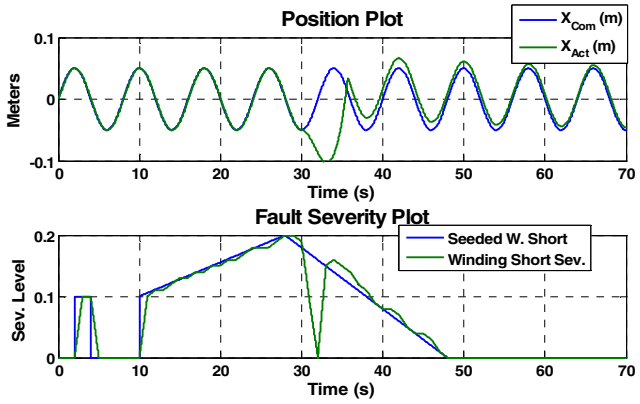

Figure 18 – Diagnosis of Winding Shorts

Similarly, friction in the motor bearings may be diagnosed using the "bearing friction level" parameter derived from the load and motor current signals. This friction is simulated as an excess torque that the motor has to overcome and is specified as a fraction of the motor's total torque capacity. Figure 19 shows that the bearing friction parameter is able to reliably assess the level of friction in the EMA motor bearings.

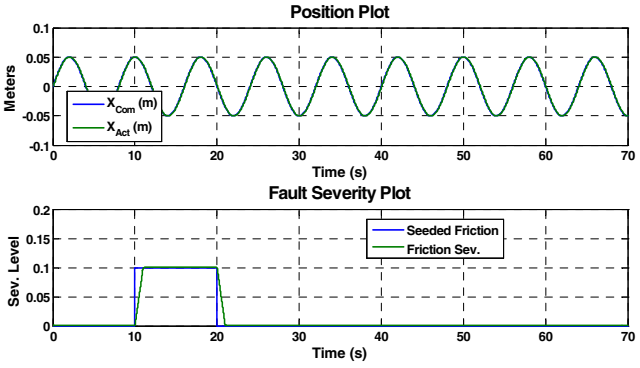

Figure 19 – Diagnosis of Bearing Friction

A position sensor (LVDT) fault was also simulated in the virtual test bed environment. This fault is simulated by a gain block, which reduces the output voltage produced by the LVDT at a given position. The LVDT fault may be diagnosed (see Figure 20) by comparing the LVDT response to the encoder output.

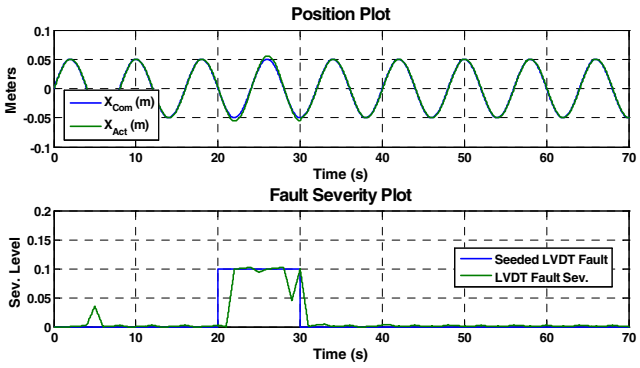

Figure 20 – Diagnosis of Position Sensor Fault

Fault separability was also assessed by simulating multiple faults in the system and observing the response of the above features. For example, Figure 21 shows the simulation of three faults simultaneously: winding shorts, seeded friction, and position sensor malfunction. As seen, the derived features are able to reliably separate these faults for the most part, with brief inaccuracies manifesting themselves when the level of the simulated fault abruptly changes. An example of this transient effect can be observed as spikes in the winding short and friction severity values at t~30 secs, when the LVDT fault is removed.

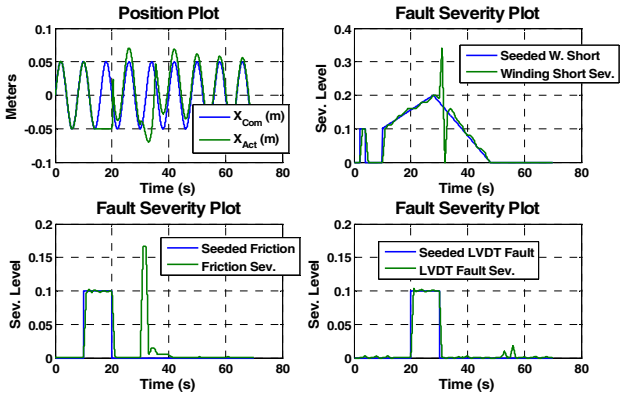

Figure 21 – Diagnosis of Multiple Faults

8. CONCLUSIONS

The work described in this paper resulted in the creation and delivery of a highly capable new test platform for the experimental consideration of electro-mechanical actuators. The high sensor density on the initial test specimen provides the opportunity to greatly enhance the understanding of healthy and faulted actuator performance. This test platform also has the potential to provide insight into the nature of the system degradation processes that contribute to EMA failure. The ability to create custom, generalized load and position profiles allows for the simulation of a variety of aircraft applications including utility actuation, flight control and propulsion applications. The design of the test

stand makes it quickly reconfigurable to accommodate new test specimens of varying configuration. This capability further extends the capability or the system for simulating and testing a variety of EMA applications.

A dynamic model of the electromechanical actuator has also been created in MATLAB®'s Simulink® environment. Since the aim was to simulate the response of the EMA to external position commands and loading patterns, a virtual test bed environment model was also created to mimic the operation of the EMA within a physical test bed. The parameters of the model, as well as the configuration and parameters of the virtual test bed, were carefully matched with the actual configuration of the electromechanical actuator test bench. The end goal of the modeling effort is to develop advanced fault diagnostics and prognostics routines for the primary failure modes of interest in EMA systems. To this end, the developed fault analysis and prognostics algorithms will be validated with data from seeded fault tests on the actuator test bench.

The concurrent, synergistic combination of experimental and analytical model-based work of these two research programs has provided a unique opportunity for the development of electro-mechanical actuator health monitoring technology. The developed techniques are expected to enhance PHM value for EMA systems, and thus increase system reliability and mitigate the effects of catastrophic EMA failures in true power-by-wire aircraft systems.

9. FUTURE WORK

The NASA EMA Test Stand has been delivered to its permanent home at the Ames Research Center, and EMA testing is scheduled in support of multiple research efforts. In addition to specific tests defined by the Ames Prognostics Center of Excellence, the test stand will be utilized by NASA partners in industry and academia. Impact Technologies will employ the test stand in support of two ongoing NASA Research Announcement (NRA) efforts. As the system is utilized for experimental research, incremental refinements are expected to the control system, software, and sensor suite. A follow-up effort is actively researching the possibility of directly instrumenting all four ball return channels with vibration measurement.

A number of tasks remain to be performed with the EMA modeling effort. Initially, the accuracy of the EMA model and the virtual test bed environment will be enhanced by making it more in line with the configuration of the actual test stand. Tuning of the parameters of the model is an additional task in this regard, and will be performed with experimental data derived from the test stand. Other fault scenarios will be investigated, and features will be identified for diagnosis of these faults. Fault classification is an important aspect of this task, and routines will be developed for accurate classification of multiple faults in the model. These routines will be verified with data from seeded fault tests on the test stand. The end goal of the effort is to develop prognostic routines to predict the useful life remaining in various components of the test stand. An issue with prognostics is the variability introduced by probabilistic and stochastic aspects that are beyond the control of the experimental parameters, such as environmental factors (dust, humidity, etc.). Approaches will be devised to take this variability into account within the overall scheme of the desired prognostic goals.

ACKNOWLEDGMENTS

The test stand development work described in this paper was conducted under subcontract number 8319-IMP-001 from QSS, Inc., NASA prime contract number NNA04AA18B. The model-based system development was conducted under NASA contract NNA08BA23C. The authors would also like to acknowledge the significant contributions of our colleagues at Impact Technologies, including Michael Ingalls, John Hertzog, Sanket Amin, and Greg Kacprzynski, without whom this work would not have been possible.

REFERENCES

[1] Jensen, S.C., Jenney, G.D., Dawson, D. "Flight Test Experience with an Electromechanical Actuator on the F-18 Systems Research Aircraft," IEEE Digital Avionics Systems Conferences, October 7-13, 2000.

[2] Blanding, D.E., "An Assessment of Developing Dual Use Electric Actuation Technologies for Military Aircraft and Commercial Application," IECEC Energy Conversion Engineering Conference, July 27 – August 1, 1997.

[3] Byington, C., Watson, M., and Edwards, D., "A Model-Based Approach to Prognostics and Health Management for Flight Control Actuators," IEEE Aerospace Conference, March 6-13, 2004.

[4] Byington, C., Watson, M., and Edwards, D., "Data-Driven Neural Network Methodology to Remaining Life Predictions for Aircraft Actuator Components," IEEE Aerospace Conference, March 6-13, 2004.

BIOGRAPHY

Matthew J. Smith *is a Senior Project Engineer at Impact*

Technologies. During his tenure with Impact, Matthew has performed multiple efforts pertaining to actuator health management, diagnostic and prognostic system development, and experimental study of faulted system response and fault progression. Previously, as a research assistant at Penn State and the NASA Glenn Research Center, Matthew performed experimental and analytical oil-free bearing analyses. Matthew received his B.S. and M.S. degrees in Mechanical Engineering from The Pennsylvania State University. His research interests include: prognostic health assessment for bearing and actuator systems, grease degradation modeling, and fault classifier development.

Carl S. Byington *is a Professional Engineer and the Director of Systems Engineering at Impact Technologies. He directs R&D in pursuit of advanced, automated systems health management for land-based, shipboard, and airborne machinery for military and commercial customers. He is Chairman of the Machinery Diagnostics & Prognostics Committee of ASME and a member of IEEE, AIAA, SAE and AHS. He has a BS degree in Mechanical Engineering from the University of Pennsylvania and an MS in Aeronautical Engineering from George Washington University, and has published over 60 papers, book chapters, magazine and journal articles related to diagnostics and prognostics technologies.*

Matthew Watson *is the Manager of Dynamic Systems at Impact Technologies. He has participated in the design of vibration algorithms, actuation systems, and dynamic systems modeling techniques for a variety of applications, including gas turbine, flight control, power transmission, drive train, electrochemical, fluid, and hydraulic systems. Prior to joining Impact, Matt worked in the Condition-Based Maintenance department of PSU-ARL, where he focused on model-based PHM development of electrochemical and fuel systems. He has co-authored over 30 papers related to advanced sensing techniques, signal processing, diagnostics and control, model-based prognostics, data fusion, and machinery health management and is co-author on 2 patents. He has a degree in Mechanical Engineering from The Pennsylvania State University.*

Sudarshan P Bharadwaj *is a Senior Project Engineer at Impact Technologies. He has been involved with a number of projects at Impact related to the health management of gas turbine engines, aircraft, and ship systems, and has considerable experience in developing diagnostics and prognostics routines for these systems. Sudarshan received his undergraduate degree in Mechanical Engineering from the Indian Institute of Technology, Madras (India), as well as Masters and Ph.D. degrees in M.E. from the Pennsylvania State University. He has published several papers in the area of prognostics and health management.*

Genna Swerdon *has been a project engineer in the Dynamic Systems group of Impact Technologies since January 2007. Her skills in data analysis and algorithm development have been used to support projects company-wide, giving her experience with prognostic health management across many mechanical systems, including generators, actuators, gearboxes, and batteries. Genna graduated from Penn State University in August 2007 with a BS in Mechanical Engineering and a minor in Engineering Mechanics. She is currently pursuing a Masters of Engineering degree in Systems Engineering from Penn State.*

Kai Goebel *received the degree of Diplom-Ingenieur from the Technische Universität München, Germany in 1990. He received the M.S. and Ph.D. from the University of California at Berkeley in 1993 and 1996, respectively. Dr. Goebel is a senior scientist at NASA Ames Research Center where he leads the Diagnostics & Prognostics groups in the Intelligent Systems division. In addition, he directs the Prognostics Center of Excellence and he is the Associate Principal Investigator for Prognostics for NASA's Integrated Vehicle Health Management Program. He worked at General Electric's Corporate Research Center in Niskayuna, NY from 1997 to 2006 as a senior research scientist. He has carried out applied research in the areas of artificial intelligence, soft computing, and information fusion. His research interest lies in advancing these techniques for real time monitoring, diagnostics, and prognostics. He holds ten patents and has published more than 100 papers in the area of systems health management.*

Edward Balaban *is a researcher in the Diagnosis and System Health group at NASA Ames Research Center. His main areas of interest are diagnostics and prognostics of physical systems. He is currently the lead for actuator prognostics with the Diagnostics & Prognostics Group in the Intelligent Systems Division. During his years at Ames he participated in research and development of diagnostic and other autonomy elements for the X-34 experimental reusable launch vehicle, International Space Station, robotic astronaut assistants, autonomous planetary drills, and the future generation of autonomous micro-spacecraft. He received the Bachelor degree in Computer Science from The George Washington University in 1996 and the Master degree in Electrical Engineering from Cornell University in 1997.*